Phase separation in paramagnetic $Eu_{0.6}La_{0.4-x}Sr_xMnO_3$

R. M. Eremina, I. I. Fazlizhanov, I. V. Yatsyk, and K. R. Sharipov
E. K. Zavoisky Physical-Technical Institute, 420029 Kazan, Russia

A. V. Pyataev
Kazan (Volga Region) Federal University, 420008 Kazan, Russia

H.-A. Krug von Nidda, N. Pascher, and A. Loidl
Experimental Physics V, Center for Electronic Correlations and Magnetism, University of Augsburg, 86135 Augsburg, Germany

K. V. Glazyrin and Ya. M. Mukovskii
Moscow State Institute of Steel and Alloys (Technological University), 119049 Moscow, Russia
(Received 18 March 2011; revised manuscript received 15 July 2011; published 18 August 2011)

We investigate the magnetic properties of the system $Eu_{0.6}La_{0.4-x}Sr_xMnO_3$ with $0.1 \leqslant x \leqslant 0.3$ by means of magnetic susceptibility and electron spin resonance measurements. Ferromagnetic resonance signals are observed in the paramagnetic regime from above the magnetic ordering temperature T_N up to approximately room temperature. This regime is characterized by the coexistence of ferromagnetic entities within the globally paramagnetic phase. The results are compared to the Griffiths scenario reported in $La_{1-x}Sr_xMnO_3$.

DOI: 10.1103/PhysRevB.84.064410 PACS number(s): 75.47.Gk, 71.70.Ej, 75.30.Et, 76.30.Fc

I. INTRODUCTION

Over the past two decades, colossal magnetoresistive (CMR) materials[1,2] have received special attention from academic and industrial researchers because of their exotic fundamental physicochemical properties as well as their technological potential in advanced applications.[3,4] Thorough investigations of the properties of CMR materials—like the hole-doped perovskite manganites[5] $R_{1-x}A_xMnO_3$, R and A being rare-earth and alkaline-earth ions, respectively—led to the discovery of many interesting physical phenomena, such as charge order as well as orbital ordering of the Mn^{3+} and Mn^{4+} ions for specific Mn^{3+}/Mn^{4+} ratios and the relationship between structural distortions and enhanced magnetic properties.[6] The transition from a paramagnetic insulating to a ferromagnetic metallic state observed in this material class is usually described within the framework of the double-exchange mechanism proposed by Zener,[7,8] in which the mobile $3d$ e_g electrons of the Mn^{3+} ions couple ferromagnetically to the localized $3d$ t_{2g} core spins due to a strong Hund's coupling.[9] However, the interplay of spin, orbital, charge, and lattice degrees of freedom gives rise to a rather complex phase diagram, which cannot be understood by the Zener mechanism only.[10]

The antiferromagnetic insulating mother compound $LaMnO_3$ ($T_N = 140$ K) is an orbitally ordered, superexchange coupled system. The orbital order in $LaMnO_3$ is induced by the cooperative Jahn-Teller effect of the Mn^{3+} ions with electronic configuration $3d^4$ (i.e., $t_{2g}^3 e_g^1$, spin $S = 2$), which, at temperatures $T < T_{JT} = 750$ K, leads to a strong orthorhombic distortion of the ABO_3 perovskite structure. Doping divalent alkali-earth ions like Sr^{2+} for La^{3+} weaken the Jahn-Teller effect, thus reducing T_{JT}, and induce a canted antiferromagnetic structure with a ferromagnetic component to the magnetization. With further increasing Sr concentration, the system passes a ferromagnetic insulating ground state centered around $x = 1/8$ before the ferromagnetic metallic phase is reached, where the cooperative Jahn-Teller effect vanishes.[11,12]

Electron spin resonance (ESR) turned out to be a very useful tool to investigate the whole phase diagram of $La_{1-x}Sr_xMnO_3$, both in the paramagnetic[13–15] and in the ordered regime.[16,17] Besides the analysis of the orbital order and the identification of the canted antiferromagnetic state, a novel triangular phase regime was discovered for single crystals with $0.075 \leqslant x \leqslant 0.175$ by means of ESR:[18] this phase is characterized by the appearance of additional resonance lines, which are observed in the ESR spectrum besides the paramagnetic resonance line at $g \approx 2$. Their intensity is several orders of magnitude lower than that of the paramagnetic line and their resonance field exhibits a pronounced anisotropy, which is independent of the microwave frequency. The temperature evolution of resonance field and intensity both resemble that of a ferromagnetic magnetization. These observations prove the coexistence of ferromagnetic entities within the globally paramagnetic phase for temperatures $T \leqslant 270$ K far above the magnetic ordering temperature. A similar triangular phase regime was recently discovered in the paramagnetic phase of $La_{1-x}Ba_xMnO_3$ single crystals with $0.1 \leqslant x \leqslant 0.2$ below 340 K.[19]

The nature of this phase can be understood in terms of Griffiths singularities arising due to the presence of correlated quenched disorder in the orthorhombic phase. The Griffiths theory was originally developed for diluted Ising ferromagnetic materials.[20] An infinite ferromagnetic cluster is formed in the paramagnetic phase below the so-called Griffiths temperature T_G down to the phase-transition temperature T_C in dependence on the dilution parameter p. Note that the ground state below T_C is a homogenous state, which is the essential difference to the usual phase separation scenarios, where the ground state is characterized by phase coexistence.

The original paper of Griffiths and subsequent works[21–25] have shown that the Griffiths phase has several characteristics. (i) The susceptibility deviates from the Curie-Weiss

predictions as $T \rightarrow T_C$ from above (at T_G). (ii) This deviation takes the form of an enhanced low field contribution due to the contribution from the ferromagnetic clusters. (iii) The deviation is suppressed in large magnetic field due to the polarization of paramagnetic spins outside the clusters; (iv) T_G can be identified as T_C of the undiluted system ($p = 1$), i.e., the maximum T_C in the phase diagram.

The features indicated above are of interest for the synthesis of new materials with Griffiths-like phases in a desired temperature range. The perovskite manganites $Eu_{1-x}Sr_xMnO_3$ are semiconductors, although they exhibit ferromagnetic behavior around $x = 0.40$ at low temperature. Only an applied magnetic field of 15 kOe induces an insulator-to-metal transition leading to a change in the resistivity exceeding six orders of magnitude at 12 K for $x = 0.40$ and 0.45 below their respective Curie temperatures of 75 and 80 K.[26] Thus, at lower external field, the quenched disorder prevails up to significantly higher Sr concentration than in $La_{1-x}Sr_xMnO_3$. This can be ascribed to the fact that Eu^{3+} ions are smaller than La^{3+} ions resulting in a stronger distortion of the perovskite lattice in addition to the Jahn-Teller effect. Quantitatively, this is described by the Goldschmidt tolerance factor $t = \frac{r_A + r_O}{\sqrt{2}(r_B + r_O)}$, where r_A, r_B, and r_O denote the radii of the A, B, and oxygen ions, respectively.[5] When t is close to 1, a cubic perovskite structure is realized; as t decreases, the lattice structure undergoes first a rhombohedral ($0.96 < t < 1$) and then an orthorhombic ($t < 0.96$) distortion. Here we investigate the related compound $Eu_{0.6}La_{0.4-x}Sr_xMnO_3$ by ESR and magnetization measurements, which allows characterizing the Griffiths phase formation in a wide concentration and temperature regime.

II. SAMPLE PREPARATION AND CHARACTERIZATION

Single-crystalline rods of $Eu_{0.6}La_{0.4-x}Sr_xMnO_3$ with $0.1 \leqslant x \leqslant 0.3$ were grown by floating-zone technique with radiation heating.[27] The feed rods were prepared from Mn_3O_4, $SrCO_3$, La_2O_3, and Eu_2O_3 powders, which were mixed in accordance with the desired metal composition. Although the crystals were multiply twinned,[28] powder x-ray diffraction prove the proper orthhorhombic structure (space group $Pbnm$). The corresponding lattice parameters a, b, and $c/\sqrt{2}$ are depicted in Fig. 1 together with those of the related system

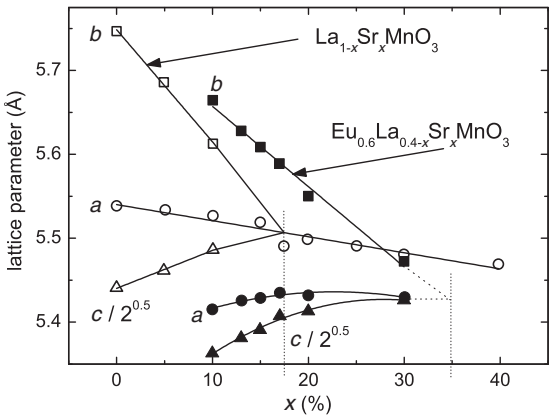

FIG. 1. Orthorhombic lattice parameters of the compounds $Eu_{0.6}La_{0.4-x}Sr_xMnO_3$ and $La_{1-x}Sr_xMnO_3$ in dependence of the strontium concentration x.

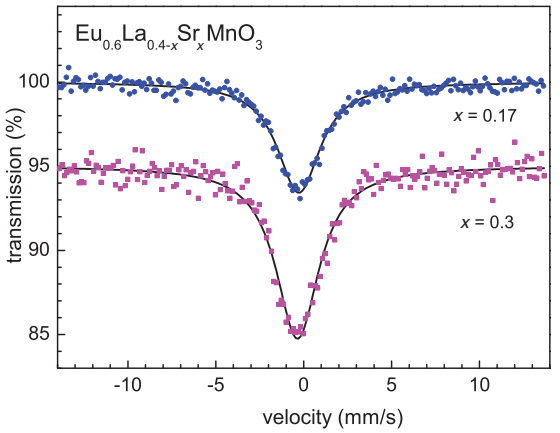

FIG. 2. (Color online) Mössbauer spectra of $Eu_{0.6}La_{0.4-x}Sr_xMnO_3$, $x = 0.17$ and 0.3, taken at room temperature 295 K. The latter spectrum is shifted by 5% downward for clarity.

$La_{1-x}Sr_xMnO_3$. It turns out that the regime of the orthorhombic phase is about twice as broad in the Eu system as compared to the reference compound.

Mössbauer spectroscopy was used to check the valency of the europium ions. Figure 2 shows typical absorption lines obtained for $x = 0.17$ and 0.3. The spectra were taken in transmission geometry at 295 K using a MS-2201 spectrometer with a $^{151}Sm_2O_3$ source of 285 MBq. The Mössbauer-absorber thickness of the sample was 25 mg Eu/cm^2. The isomer shift value $\delta_{\text{eff}} = -0.33 \pm 0.04$ mm/s, determined with respect to Eu_2O_3 at $T = 295$ K, corresponds to a trivalent charge state Eu^{3+}, i.e., the holes are induced by the Sr^{2+} ions, only.

Magnetization measurements were performed using a superconducting quantum interference device (SQUID) magnetometer MPMS5 (Quantum Design) in magnetic fields up to $H \leqslant 50$ kOe for the temperature regime $1.8 \leqslant T \leqslant 400$ K. The ESR measurements were carried out in a Bruker ELEXSYS E500-CW spectrometer working at X-band (9.4 GHz) and Q-band (34 GHz) frequencies equipped with continuous-flow He cryostats (Oxford Instruments) covering the temperature range $4.2 \leqslant T \leqslant 300$ K. Due to the lock-in amplification with field modulation, the ESR spectra record the field derivative of the microwave absorption dependent on the external static field.

III. RESULTS

A. Magnetization

Figure 3 shows the field-dependent magnetization loops of all compounds under consideration taken at $T = 2$ K. For $x = 0.1$, one observes a hysteresis loop with a coercive field of about 5 kOe and a remnant moment of approximately $0.6\mu_B$. With increasing magnetic field, the magnetization exhibits a saturation behavior to a value close to $2\mu_B$, i.e., far below the possible maximum saturation value of $3.9\mu_B$. This resembles the characteristics of a canted antiferromagnet like that observed in $La_{1-x}Sr_xMnO_3$ for $x < 0.1$.[12] With increasing strontium concentration, the width of the hysteresis decreases and nearly vanishes at $x = 0.2$. At the same time, the magnetic moment determined at the maximum field of 50 kOe (triangles in the upper frame of Fig. 5) increases linearly with

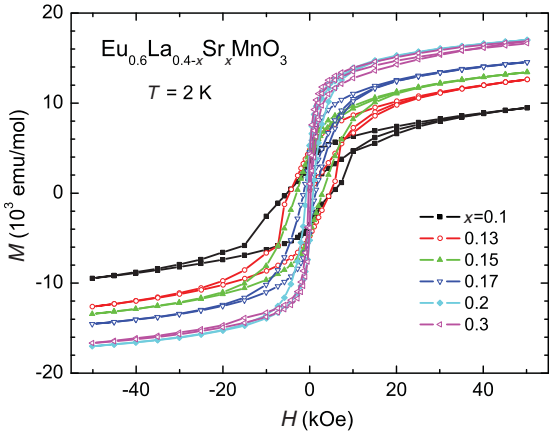

FIG. 3. (Color online) Magnetization M of $Eu_{0.6}La_{0.4-x}Sr_xMnO_3$ dependent on magnetic field H at $T = 2$ K.

x, reaches about $3\mu_B$ per formula unit for $x = 0.2$, and remains constant for larger x. In contrast to $La_{1-x}Sr_xMnO_3$, where full ferromagnetic alignment is already approached at $x = 0.1$, this value of the magnetic moment is still significantly below the expected ferromagnetic saturation value of all manganese spins indicated in Fig. 5 as a dotted line. This discrepancy can be ascribed to the van Vleck contribution of the Eu^{3+} spins, which also influences the effective paramagnetic moment, as documented in the following.

Figure 4 illustrates the temperature dependence of the magnetic susceptibility $\chi = M/H$ measured in a low magnetic field of $H = 10$ Oe after field cooling (FC) and zero-field cooling (ZFC), as well as the inverse susceptibility $1/\chi$ taken also in a high field of $H = 10$ kOe. Starting from the high-field data, one observes a Curie-Weiss law $\chi^{-1} = C^{-1}(T - \Theta_{CW})$ at elevated temperatures, which allows determining the Curie-Weiss temperature Θ_{CW} from the intercept point with the abscissa and the effective paramagnetic moment $\mu_{eff} = \sqrt{3k_BC/N_A}$ from the Curie constant C, where k_B and N_A denote the Boltzmann constant and Avogadro number, respectively. As one can see in Fig. 5, both parameters are practically independent on the Sr concentration x: The Curie-Weiss temperature is positive, slightly above 100 K in accordance with the ferromagnetic superexchange between the manganese ions present in the ab plane. The effective moment $\mu_{eff} \approx 6\mu_B$ is significantly enhanced with respect to the theoretically expected paramagnetic moment of the manganese spins, i.e., $\mu^2_{Mn} = (1-x)\mu^2_{3+} + x\mu^2_{4+}$, indicated as a dashed line in the upper frame of Fig. 5. As in pure $EuMnO_3$, this enhancement results from the non-negligible van Vleck contributions of the excited spin states of the Eu^{3+} ions.[29]

The measurements at low field serve for a correct identification of the magnetic ordering temperature T_N: especially the ZFC susceptibility reveals a pronounced peak at T_N. Below T_N, FC and ZFC measurements differ strongly due to the domain structure of the ordered phase. Notably, for all Sr concentrations under consideration, except $x = 0.3$, even above T_N clear differences show up, which indicate the existence of ferromagnetic regions in the paramagnetic regime below a certain temperature $T_G \approx 270$ K, like in $La_{1-x}Sr_xMnO_3$ for $0.075 \leqslant x \leqslant 0.15$, where a full Griffiths-phase triangle could be detected.[18] In ferro- or

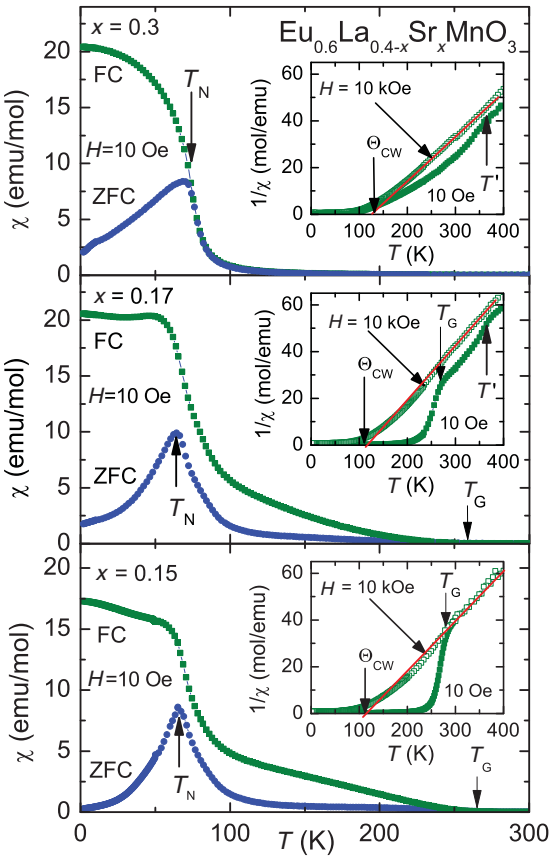

FIG. 4. (Color online) Temperature dependence of the magnetic susceptibility $\chi = M/H$ of $Eu_{0.6}La_{0.4-x}Sr_xMnO_3$ for three representative compounds $x = 0.15$, 0.17, and 0.3 measured at low magnetic field $H = 10$ Oe field cooled (FC, squares) and zero-field cooled (ZFC, circles). Insets: Inverse FC susceptibilities taken both at high field $H = 10$ kOe (open squares) and low field $H = 10$ Oe (solid squares).

ferrimagnets just below the Curie temperature, a similar splitting of FC and ZFC susceptibilities can be observed for polycrystalline material in contrast to perfect single crystals due to pinning of the magnetic domain walls by grain boundaries, like, e.g., in $FeCr_2S_4$.[30] In the present case of $Eu_{0.6}La_{0.4-x}Sr_xMnO_3$, such pinning arises from the granular structure of the ferromagnetic regions fixed by quenched disorder in the paramagnetic matrix.

For $0.17 \leqslant x \leqslant 0.3$, another weaker anomaly shows up close to $T' \approx 350$ K corresponding to the maximum ferromagnetic transition temperature observed in $La_{1-x}Sr_xMnO_3$ for $x \approx 0.4$.[31]

B. Electron spin resonance

Further important microscopic information is obtained by means of ESR. Figure 6 shows characteristic ESR spectra obtained at X-band and Q-band frequency for $x = 0.13$ at intermediate temperature between T_N and T_G, as identified from the susceptibility measurements. For both frequencies, besides the paramagnetic resonance centered at a g value close to $g = 2$ due to the majority of Mn^{3+} and Mn^{4+} spins,[13] a pronounced second line shows up at a resonance field about 1 kOe lower than the paramagnetic line. Already

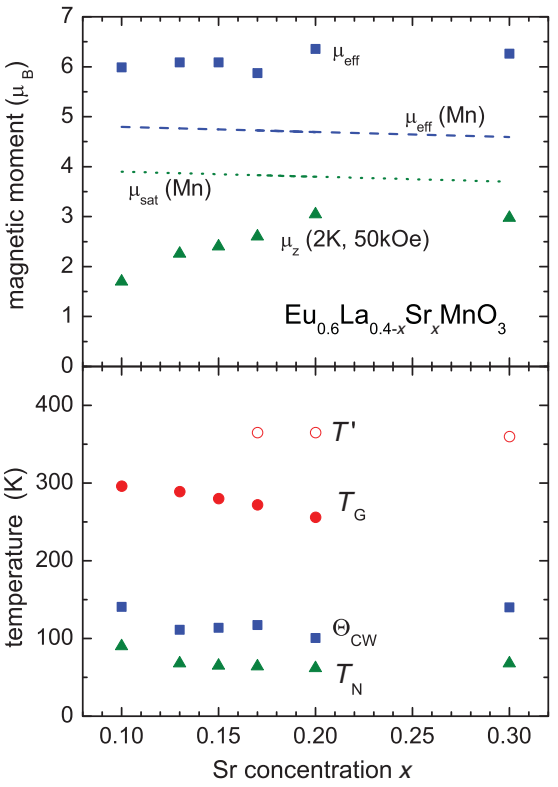

FIG. 5. (Color online) Upper frame: effective paramagnetic moments μ_{eff} (squares) determined from the slope of the inverse susceptibilities at high temperatures and z component of the magnetization μ_z (triangles) in the ordered phase taken at $T = 2$ K and $H = 50$ kOe. The dashed and dotted lines indicate the theoretically calculated effective and saturated moments, respectively. Lower frame: Curie-Weiss temperature Θ_{CW} (squares), magnetic ordering temperature T_{N} (triangles), and possible Griffiths temperatures T_{G} (solid circles) and T' (open circles) dependent on the Sr concentration.

from the comparison of the spectra at two frequencies the ferromagnetic character of this second line is visible. While the intensity of the paramagnetic line is expected to increase linearly with the field like the paramagnetic magnetization, the ferromagnetic signal intensity should be field-independent as soon as the magnetization is saturated. Indeed, at Q-band frequency, the low-field line appears to be suppressed with respect to the paramagnetic resonance signal, when comparing with the measurements at X band. Note that, due to the different microwave cavities used in X and Q band, both spectra have been just normalized to the paramagnetic resonance signals, i.e., in absolute magnitude the paramagnetic signal is increasing linearly with increasing frequency, while the FMR-signal intensity does not change.

Such ferromagnetic resonance signals were observed in the paramagnetic regime above T_{N} in single crystals with Sr concentrations $x = 0.13, 0.15, 0.17$, and 0.2. They all separate from the paramagnetic signal below 270 K, corroborating the temperature scale T_{G} above T_{C}, which is almost independent of x. Figure 7 illustrates the temperature dependence of the EPR line position in X and Q band. The difference between the position of the ferromagnetic resonance line in low fields and the paramagnetic resonance is independent of the microwave frequency at which the experiment is

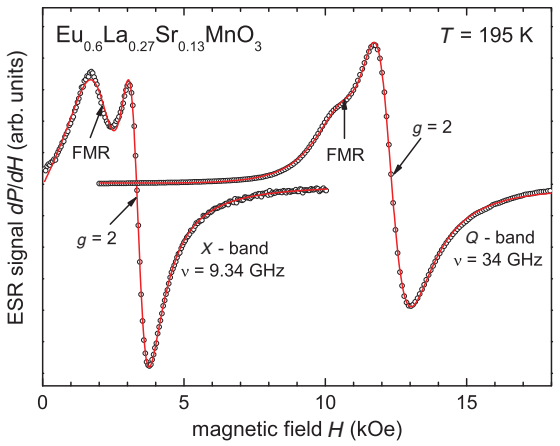

FIG. 6. (Color online) EPR spectra in $Eu_{0.6}La_{0.27}Sr_{0.13}MnO_3$ at a temperature $T = 195$ K. The spectra consist of a paramagnetic resonance signal with $g \approx 2$ and a ferromagnetic resonance (FMR) signal at lower resonance field. The solid line represents a fit with the sum of two Dysonian lines.[32]

carried out and amounts to about 1 kOe. A similar splitting was observed for the $La_{1-x}Sr_xMnO_3$ and $La_{1-x}Ba_xMnO_3$ single crystals for the magnetic field applied within the ab plane.[18,19] Note, however, that the strong anisotropy observed for the ferromagnetic line in those compounds could not be detected in $Eu_{0.6}La_{0.4-x}Sr_xMnO_3$. This probably can be explained by the multiple twinning of the single crystals under investigation. Therefore, the spectra are similar to those of powder samples, where the average of a dominantly uniaxial anisotropy pronounces the perpendicular component of the orientation dependence.

The FMR intensity in the compounds under consideration is by orders of magnitude larger than in $La_{1-x}Sr_xMnO_3$ and the width of the temperature regime $T_{\text{N}} \leqslant T \leqslant T_{\text{G}}$ is about 200 K. Thus it is possible to follow the temperature dependence of the ferromagnetic resonance line over a broad temperature range: the temperature dependence of the double integrated intensities of both paramagnetic and ferromagnetic resonance signals obtained at X- and Q-band frequency is

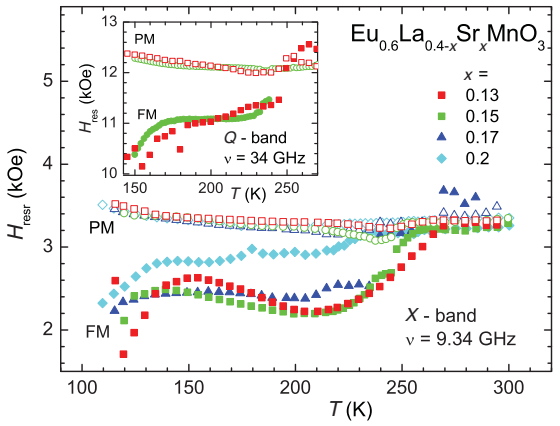

FIG. 7. (Color online) Temperature dependence of the resonance fields of paramagnetic (open symbols) and ferromagnetic (solid symbols) contributions in the spectrum of $Eu_{0.6}La_{1-x}Sr_xMnO_3$ determined at 9.34 (main frame) and 34 GHz (inset).

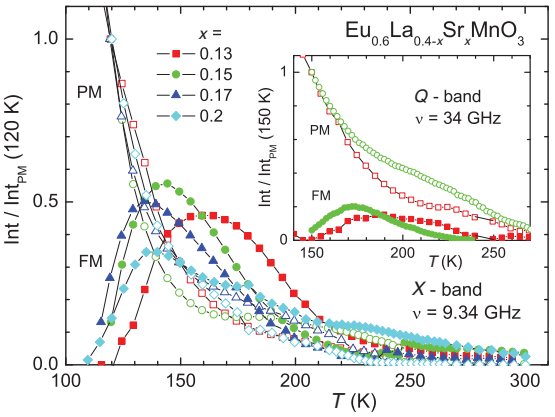

FIG. 8. (Color online) Temperature dependence of the paramagnetic (open symbols) and ferromagnetic (solid symbols) resonance intensities in $Eu_{0.6}La_{0.4-x}Sr_xMnO_3$ at 9.34 (main frame) and 34 GHz (inset).

presented in Fig. 8. In all compounds under consideration the FMR intensity first clearly increases with decreasing temperature, passes a maximum, and then decreases again. The behavior of paramagnetic signal intensity is close to a Curie-Weiss law with deviations indicating additional ferromagnetic contributions, which cannot be separated due to the multiple twinning. The maxima of the ferromagnetic intensity appear dependent on x between 140 and 160 K at X-band frequency and are shifted by approximately 30 K upward at Q-band frequency.

Besides these well-resolved ferromagnetic signals, additional weaker ferromagnetic resonance features are observed on the paramagnetic resonance line even above T_G, which are not shifted from $g \approx 2$ and, thus, cannot be well separated.

IV. DISCUSSION

The new phase regime between $T_N \leqslant T \leqslant T_G$ discovered in $Eu_{0.6}La_{0.4-x}Sr_xMnO_3$ exhibits the coexistence of paramagnetic and ferromagnetic resonance lines already far above the actual magnetic ordering transition at T_N, which was identified as a typical feature of a Griffiths phase in the related compound $La_{1-x}Sr_xMnO_3$. However, as one can see in Fig. 5, the triangular shape expected for the Griffiths phase regime does not seem to be realized in the present compound. Instead of an increase of the magnetic ordering temperature T_N with increasing Sr concentration x, which finally should meet the Griffiths temperature T_G at a well-defined x value representing the ideal ferromagnetic system in this series, both T_N as well as T_G change only weakly with x, while T_G disappears somewhere for $0.2 < x < 0.3$. As the intensity of the corresponding ferromagnetic signal decreases already from $x = 0.17$ to $x = 0.2$, the ferromagnetic entity presumably further shrinks gradually above $x = 0.2$ due to the gradual reduction of quenched disorder with increasing Sr concentration and finally becomes undetectable. To understand this observation, we have to recall the mechanism of quenched disorder responsible for the generation of the Griffiths phase.[18] In $La_{1-x}Sr_xMnO_3$, the source of disorder is the random substitution of La^{3+} ions by Sr^{2+} ions of different size and valence. The probability for the existence of a ferromagnetic bond increases with the Sr concentration x, because the increasing number of Mn^{3+}-Mn^{4+} pairs enhances the double-exchange driven ferromagnetic interaction. Due to the static Jahn-Teller distortion of the Mn^{3+} ions, which are in majority, the non-Jahn-Teller active Mn^{4+} ions and the corresponding bonds can be regarded as fixed within the lattice as long as the cooperative Jahn-Teller distortion persists and the compound remains semiconducting. This situation is termed as quenched disorder of the ferromagnetic bonds.

In Brays generalization of Griffiths concept to ferromagnetic systems with an arbitrary distribution of bond strengths, the Griffiths temperature scale T_G is not just the critical temperature of the pure ferromagnetic system, but represents the maximum critical temperature among all configurations compatible with the static nature of disorder.[21] In $La_{1-x}Sr_xMnO_3$, the static disorder is annealed above $x = 0.16$ as a consequence of the transition from the Jahn-Teller distorted orthorhombic to the rhombohedral phase, i.e., as the random locations of the ferromagnetic bonds begin to fluctuate concomitantly with the fluctuating lattice distortions. The additional substitution of La^{3+} by the smaller isovalent Eu^{3+} ions further stabilizes the orthorhombic distortion and concomitant quenched disorder up to even higher Sr concentrations x. At the same time, T_G still stays at the value of the Eu^{3+}-free system, which on random substitution of Eu^{3+} locally remains the maximum magnetic ordering temperature, because substitution of La^{3+} by smaller rare-earth ions generally reduces the magnetic ordering temperature.[33] This is caused by the enhanced tilting of the MnO_6 octahedra, which results in an increasing importance of antiferromagnetic next-nearest-neighbor interactions competing with the nearest-neighbor superexchange within the ferromagnetic ab planes of the A-type antiferromagnetic structure. This weakening of the effective magnetic interaction promotes a tendency toward frustration and complex spin states. Therefore, in the substitution series under consideration, T_N never reaches T_G. To investigate the continuous evolution of the Griffiths triangle, a substitution series $Eu_xLa_{0.84-x}Sr_{0.16}MnO_3$ would be of high interest.

The second important observation of the present study concerns the fact that the intensity of the ferromagnetic signal decreases and goes to zero on approaching the ordering temperature. This has not been explicitly worked out in previous studies of related systems,[18,19] because there the intensity of the ferromagnetic line was too weak to make definite statements when the main paramagnetic line became dominant near T_N. In $Eu_{0.6}La_{0.4-x}Sr_xMnO_3$, both the paramagnetic and the ferromagnetic signal are of comparable intensity. Therefore, the intensity of both lines can be easily evaluated. On the base of our assumption[18] that the shift of the ferromagnetic line results from the demagnetization which is related to the probably pancake-like shape of the ferromagnetic clusters, the reduction of the intensity of the ferromagnetic line on approaching magnetic order results from the coagulation of the clusters, when the paramagnetic regions in between become strongly magnetized, which in turn strongly changes the demagnetization. In this context, the observed frequency dependence of the intensity maxima results from the larger magnetic polarization of the paramagnetic regions at about

$H = 10$ kOe in Q band, compared to $H = 2.5$ kOe in X band, which results in a coagulation of the ferromagnetic clusters already at higher temperatures. The existence of pancake-shaped clusters even within the ordered phase was recently confirmed by neutron-scattering experiments.[34]

The third point to be mentioned is the appearance of a second Griffith-like temperature T', which is close to the maximum Curie temperature T_C in the phase diagram of $La_{1-x}Sr_xMnO_3$ at $x \approx 0.4$, i.e., in the ferromagnetic metallic regime. The susceptibility exhibits a weak ferromagnetic contribution, which is accompanied by an additional resonance signal in the ESR spectrum. Interestingly, this resonance line does not shift from the position of the paramagnetic resonance close to $g = 2$. This indicates that the ferromagnetic regions formed below T' are rather isotropic and develop spherical shapes. In contrast to the phase regime limited by T_G, one can expect that the clusters formed below T' are not governed by quenched disorder, but rather exhibit metallic character. Again a full triangular phase regime cannot be observed, but for a more detailed study of the evolution of this phase, a substitution series like $Eu_xLa_{0.6-x}Sr_{0.4}MnO_3$ should be investigated.

V. SUMMARY

In conclusion, the ESR and magnetic susceptibility studies revealed Griffiths-like phase regimes in the paramagnetic state of $Eu_{0.6}La_{0.4-x}Sr_xMnO_3$ with $0.1 \leqslant x \leqslant 0.3$. These regimes are characterized by distinct ferromagnetic contributions to the paramagnetic susceptibility and by the coexistence of ferromagnetic and paramagnetic ESR signals for temperatures $T_N \leqslant T \leqslant T_G \approx 270$ K and/or $T' \approx 350$ K. Although the triangular shape expected for a Griffiths phase in the x-T diagram is not completed in the present substitutional series, the observed transition temperatures T_G and T' correspond to the Curie temperature at the boundary between the orthorhombic and the rhombohedral structural phase and to the maximum Curie temperature in the rhombohedral phase of the related compound $La_{1-x}Sr_xMnO_3$, respectively. Thus the results of the present study may serve as the starting point for more detailed investigations under variation of the europium concentration at fixed strontium content, which should allow one to close the Griffiths triangles for both T_G and T'.

ACKNOWLEDGMENTS

We are very grateful to Anna Pimenov for SQUID measurements. This work was partially supported by the Deutsche Forschungsgemeinschaft (DFG) within the Transregional Collaborative Research Center TRR 80 (Augsburg, Munich) and by the Russian Federal Program, Grant No. 02.740.11.0103.

[1] R. M. Kusters, D. A. Singleton, R. Mcgreevy, and W. Hayes, Physica B **155**, 362 (1989).
[2] R. von Helmolt, J. Wecker, B. Holzapfel, L. Schultz, and K. Samwer, Phys. Rev. Lett. **71**, 2331 (1993).
[3] Ch. Jooss, L. Wu, T. Beetz, R. F. Klie, M. Beleggia, M. A. Schofield, S. Schramm, J. Hoffmann, and Y. Zhu, Proc. Natl. Acad. Sci. USA **104**, 13597 (2007).
[4] V. N. Krivoruchko, M. A. Marchenko, and Y. Melikhov, Phys. Rev. B **82**, 064419 (2010).
[5] G. H. Jonker and J. H. van Santen, Physica **16**, 337 (1950).
[6] V. M. Loktev and Yu. G. Pogorelov, Low Temp. Phys. **26**, 171 (2000) [Fiz. Nizk. Temp. **26**, 231 (2000)].
[7] C. Zener, Phys. Rev. **82**, 403 (1951).
[8] P. W. Anderson and H. Hasegawa, Phys. Rev. **100**, 675 (1955).
[9] P. G. de Gennes, Phys. Rev. **118**, 141 (1960).
[10] J. B. Goodenough, A. Wold, R. J. Arnott, and N. Menyuk, Phys. Rev. **124**, 373 (1961).
[11] A. K. Bogush, V. I. Pavlov, and L. V. Balyko, Cryst. Res. Technol. **18**, 589 (1983).
[12] M. Paraskevopoulos, F. Mayr, J. Hemberger, A. Loidl, R. Heichele, D. Maurer, V. Müller, A. A. Mukhin, and A. M. Balbashov, J. Phys. Condens. Matter **12**, 3993 (2000).
[13] V. A. Ivanshin, J. Deisenhofer, H.-A. Krug von Nidda, A. Loidl, A. A. Mukhin, A. M. Balbashov, and M. V. Eremin, Phys. Rev. B **61**, 6213 (2000).
[14] J. Deisenhofer, B. I. Kochelaev, E. Shilova, A. M. Balbashov, A. Loidl, and H.-A. Krug von Nidda, Phys. Rev. B **68**, 214427 (2003).
[15] G. Alejandro, M. C. G. Passeggi, D. Vega, C. A. Ramos, M. T. Causa, M. Tovar, and R. Senis, Phys. Rev. B **68**, 214429 (2003).
[16] A. Pimenov, M. Biberacher, D. Ivannikov, A. Loidl, V. Yu. Ivanov, A. A. Mukhin, and A. M. Balbashov, Phys. Rev. B **62**, 5685 (2000).
[17] D. Ivannikov, M. Biberacher, H.-A. Krug von Nidda, A. Pimenov, A. Loidl, A. A. Mukhin, and A. M. Balbashov, Phys. Rev. B **65**, 214422 (2002).
[18] J. Deisenhofer, D. Braak, H.-A. Krug von Nidda, J. Hemberger, R. M. Eremina, V. A. Ivanshin, A. M. Balbashov, G. Jug, A. Loidl, T. Kimura, and Y. Tokura, Phys. Rev. Lett. **95**, 257202 (2005).
[19] R. M. Eremina, I. V. Yatsyk, Ya. M. Mukovski, H.-A. Krug von Nidda, and A. Loidl, JETP Lett. **85**, 51 (2007) [Pis'ma Zh. Eksp. Teor. Fiz. **85**, 57 (2007)].
[20] R. B. Griffiths, Phys. Rev. Lett. **23**, 17 (1969).
[21] A. J. Bray, Phys. Rev. Lett. **59**, 586 (1987).
[22] J. M. de Teresa, M. R. Ibarra, P. A. Algarabel, C. Ritter, C. Marquina, J. Blasco, J. Garcia, A. del Moral, and Z. Arnold, Nature (London) **386**, 256 (1997).
[23] J. Burgy, M. Mayr, V. Martin-Mayor, A. Moreo, and E. Dagotto, Phys. Rev. Lett. **87**, 277202 (2001).
[24] M. B. Salamon, P. Lin, and S. H. Chun, Phys. Rev. Lett. **88**, 197203 (2002).
[25] E. Dagotto, New J. Phys. **7**, 67 (2005).
[26] S. Nakamura, Y. Tadokoro, Y. J. Shan, and T. Nakamura, J. Phys. Soc. Jpn. **68**, 1485 (1999).
[27] Ya. Mukovskii, V. Arkhipov, A. Arsenov, N. Bebenin, V. Dyakina, V. Gaviko, A. Korolev, S. Karabashev, V. Mashkautsan, and E. Neifeld, J. Alloys Compd. **326**, 108 (2001).

[28]R. Tamazyan, N. Rotiroti, S. van Smaalen, Ya. Mukovskii, and A. Arsenov, Acta Crystallogr. Sect. C **62**, i3 (2006).
[29]J. Hemberger, F. Schrettle, A. Pimenov, P. Lunkenheimer, V. Yu. Ivanov, A. A. Mukhin, A. M. Balbashov, and A. Loidl, Phys. Rev. B **75**, 035118 (2007).
[30]V. Tsurkan, V. Fritsch, J. Hemberger, H.-A. Krug von Nidda, N. Büttgen, D. Samusi, S. Körner, E.-W. Scheidt, S. Horn, R. Tidecks, and A. Loidl, J. Phys. Chem. Solids **66**, 2036 (2005).
[31]J. Hemberger, A. Krimmel, T. Kurz, H.-A. Krug von Nidda, V. Yu. Ivanov, A. A. Mukhin, A. M. Balbashov, and A. Loidl, Phys. Rev. B **66**, 094410 (2002).
[32]Janhavi P. Joshi and S. V. Bhat, J. Magn. Reson. **168**, 284 (2004).
[33]T. Goto, T. Kimura, G. Lawes, A. P. Ramirez, and Y. Tokura, Phys. Rev. Lett. **92**, 257201 (2004).
[34]S. Petit, M. Hennion, F. Moussa, D. Lamago, A. Ivanov, Y. M. Mukovskii, and D. Shulyatev, Phys. Rev. Lett. **102**, 207201 (2009).